

ANDRZEJ OSAK\*

## RELAXATION CURRENTS IN THE NON-MORPHOTROPIC REGION OF PZT-PFS FERROELECTRIC CERAMICS

### PRĄDY RELAKSACYJNE W OBSZARZE POZAMORFOTROPOWYM FERROELEKTRYCZNEJ CERAMIKI PZT-PFS

#### Abstract

Studies on the dielectric relaxation currents in the non-morphotropic region of PZT-PFS are presented. Transient polarization and depolarization currents were measured at different poling fields (0.02–20 kV/cm) and different temperatures (77–473 K). The activation energies were calculated. The defect dipole complex ( $\text{Fe}_{\text{Tizr}}-\text{V}_\text{O}$ ) and reorientation cluster dipole models are proposed to explain the observed relaxation behaviour in PZT-PFS.

*Keywords: ferroelectric ceramics, PZT-PFS, relaxation currents*

#### Streszczenie

W artykule przedstawiono badania prądów realaksacji dielektrycznej w PZT-PFS dla składów leżących poza morfotropową granicą faz. Zostały zmierzone prądy polaryzacji i depolaryzacji dla różnych wartości pola polaryzacji (0.02–20kV/cm) i temperatur (77–473 K). Wyznaczono energie aktywacji dla różnych próbek. Dla wyjaśnienia relaksacyjnego charakteru zjawisk w PZT-PFS został zaproponowany model oparty o zespoły defektów dipolowych ( $\text{Fe}_{\text{Tizr}}-\text{V}_\text{O}$ ) i reorientacje klastrów dipoli.

*Słowa kluczowe: ceramika ferroelektryczna, PZT-PFS, prądy relaksacji*

\* Institute of Physics, Faculty of Physics Mathematics and Computer Science, Cracow University of Technology; andrzej.osak@if.pk.edu.pl.

## 1. Introduction

Study of transient decaying currents is a very useful method for the determination of slow polarization and depolarization processes in ferroelectric materials. Such a study provides some insights into the microscopic mechanisms of polarization and depolarization processes and can explain aging, memory effects, domain wall motion, and the dynamics of dipoles, ions and electrons [1–4].

The results of measurements of the polarization and depolarization currents in the morphotropic region have previously been described in [5]. The present paper reports some additional studies on depolarization currents in the non-morphotropic region. Details of the experimental procedure and sample characterization are presented in [5].

Samples with circular silver electrodes with an area of 0.36 cm<sup>2</sup> and thickness 0.5 mm are used in all experiments. The samples Pb[(Fe<sub>1/3</sub>Sb<sub>2/3</sub>)<sub>x</sub>Ti<sub>y</sub>Zr<sub>z</sub>]O<sub>3</sub> with  $x + y + z = 1$ ,  $x = 0.1$  and  $y = 0.43$  and  $y = 0.47$  compositions were subjected to an electric field and the decaying current was measured under different strengths of the applied field. After poling, the applied field was removed and the sample was short circuited via a current-measuring 6517A Keithley electrometer until the reverse depolarization current had decayed.

## 2. Results

The relaxation behavior in PZT+PFS was studied for various poling fields, polarization times and temperatures. Fig. 1 shows the time dependence of the depolarization currents which were recorded after various poling times, i.e. 10<sup>2</sup>, 10<sup>3</sup> and 10<sup>4</sup> s. The results are shown as the log-log scale plots. Initially, there was little difference between the curves, but at longer times, that difference increased. The depolarization current curves for polarization times 10<sup>4</sup> s and longer have tendency to coincident.

In Fig. 2a, the depolarization current for different poling field measured at 298 K, are plotted. It is evident that at a low poling field, one observes a linear dependence relaxation current in the probe field, whereas for higher poling fields, a rapid increase of nonlinearity appears and, simultaneously, the depolarization time becomes longer than 10<sup>4</sup> s. In Fig. 2b, the time dependences of depolarization currents, measured at 77 K, are shown. At lower poling fields, the depolarization currents are proportional to the electric field strength, but at higher fields, a non-linear behaviour is observed. However, the onset of the non-linear dependence begins at lower *poling* fields than in the case of higher temperature (298 K).

In Fig. 3, the polarization  $J_p$ , steady state  $J_s$  and depolarization  $J_d$  currents are presented for sample with  $y = 0.47$ . The charging currents at any time are the sum of the current due to both the decaying polarization current and the steady state conduction current:

$$J_c = J_p + J_s \quad (1)$$

At 298 K, the decaying currents are given for poling fields 0.02 (plot C) and 5 kV/cm (plot A). For low poling fields (0.02 kV/cm), the polarization and depolarization currents have approximately the same values at the same time (see Fig. 3, plot C, curves  $J_p$  and  $J_d$ ). Whereas for higher fields 5 kV/cm, the depolarization current is lower than the polarization current (see Fig. 3, plot A curves  $J_p$  and  $J_d$ ). At higher temperature (453 K), for the 0.02 kV/cm poling

field, the decaying polarization and depolarization currents have almost equal values at the same time (see Fig. 3, plot B, curves  $J_p$  and  $J_d$ ) and the observed curves are mirror images of each other. Typical examples of the depolarization currents, measured under a low poling field (0.02 kV/cm) over the time period 1–10<sup>4</sup> s for selected temperatures for samples  $y = 0.43$  and  $y = 0.47$ , are shown in Figs. 4a and 4b, respectively. The shape of the relaxation currents presented in Figs. 4a and 4b indicates the existence of two time-dependent relaxation processes, both obeying the well-known Jonscher-Dissado-Hill fractional power law:

$$J(t) = \frac{A(t)}{\left(\frac{\tau}{\tau_0}\right)^n + \left(\frac{\tau}{\tau_0}\right)^m} \quad (2)$$

where  $\tau_0 = \omega_0^{-1}$  is the relaxation time for which the loss peak appears.

The relaxation of depolarization currents proceed faster, i.e. over a time shorter than the relaxation time  $\tau_0$  with the form  $t^{-n}$  and slower at times longer than  $\tau_0$  with the form  $t^{-m}$  [7]. Values of the exponents  $n$  and  $m$ , depending on temperature, are listed in Table 1. The insets in Figs. 4 a and b show the temperature dependence of the  $\log \tau_0^{-1}$  vs  $1000/T$ . The activation energies calculated from the slope of this dependence are listed in Table II, along with the activation energies obtained from the electric conduction.

### 3. Discussion

1. The polarization and depolarization current decays at low ( $\sim 0.02$  kV/cm) and high poling fields ( $\sim 20$  kV/cm) as well as for different poling time were measured. The results presented in Fig. 1 show that, for a short poling time, only relaxation processes with short relaxation times are developed. Poling times of at least the order 10<sup>4</sup> s are needed to initiate all various polarization processes with long relaxation times, both at high and low temperatures. For a weak poling field ( $\sim 0.2$  kV/cm), there is no difference between polarization and depolarization currents, as shown in Fig. 3, plots B and C. This means that the reorientation of dipoles and domain wall motion is reversible and that the ferroelectric under study behaves as a linear dielectric. The onset of irreversible motion of the domain walls begins at higher fields [8]. In this range of poling field, the depolarization current at any time is less than the polarization current (see Fig. 3, plot A) and the remnant polarization is induced. At very high poling fields (20 kV/cm; Fig. 2a), the space charge appears providing an additional contribution to the total discharge current [5, 6].

2. The properties of the PZT compounds are strongly altered by point defects. In the case of  $\text{Pb}(\text{Zr,Ti})\text{O}_3$  modified by FeSb ions, randomly distributed  $\text{Ti}^{4+}$ ,  $\text{Zr}^{4+}$ ,  $\text{Fe}^{3+}$  ions on the B site of the perovskite structure are created. The group of octahedrons with identical B site ions  $(\text{BO}_6)_n$  gives rise to a micro-region (cluster) with a large number of locally interacting dipoles. The nanometer size clusters with various composition have dipole moments undergoing the thermal fluctuation between equivalent positions. Between clusters, some coupling interaction occurs leading to partial long-range regularity. Longer relaxation times are associated with relaxation due to the cooperative motion of the group of clusters (micro-regions) [10, 11]. The observed, in initial time, the power law dependence  $J_p(t) \sim t^{-n}$  may be

explained take into account dipol-dipol and ion-ion interactions. As it was shown in paper [12] such interaction leads to the generation low-energy correlated states. The density of this low-energy excitation gives rise to the infrared divergence response function  $t^{-n}$ .

3. In the case of PZT with  $\text{Fe}^{3+}$  ions, three  $\text{Fe}_{\text{TiZr}}-\text{V}_{\text{O}}$  defect complexes could be formed depending on whether the oxygen atoms were removed or not [13, 14]. The energy barriers for reorientation of these defect complexes depend on the position of oxygen vacancies with respect to iron atoms [13, 14]. In the tetragonal phase of the PZT, there are two types of oxygen atoms – the oxygen atoms bonded to two Ti atoms in ab planes [O(2)] and the oxygen atoms in the O-Ti-O chains in c directions [O(1)]. Therefore, one may expect three kinds of defect complexes. The Debye-type relaxation peaks (see Figs. 4a and b), observed, in both samples, can be attributed to the reorientation defect complexes formed by the oxygen vacancies. Activation energies obtained from relaxation times (see Table 2) approximately equals to the energy barrier of the defect dipole rotation calculated in paper [13, 14].

Table 1

Values of power exponents  $n$  and  $m$  for samples with  $y = 0.43$  and  $y = 0.47$ 

$y = 0.43$			$y = 0.47$		
$T$ [K]	$n$	$m$	$T$ [K]	$n$	$m$
298	0.72	1.17	298	0.73	1.19
343	0.68	1.18	423	0.72	1.22
398	0.62	1.19	473	0.70	1.28

Table 2

Activation energies obtained from the measurements of relaxation times  $E_r$  and electrical conduction  $E_c$  [15]

composition	$E_r$ [eV]	$E_c$ [eV]
$y = 0.43$	0.34	0.37
$y = 0.47$	0.16	0.17

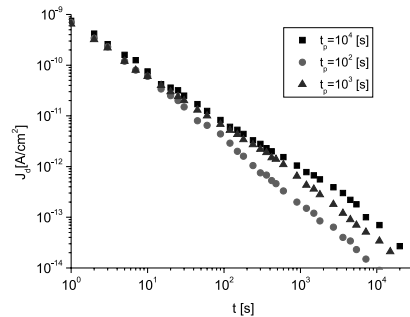


Fig. 1. Time-dependence of depolarization currents ( $J_d$ ) for various poling times ( $t_p$ ) measured at 298 K for sample with  $y = 0.47$ . Poling field: 0.02 kV/cm

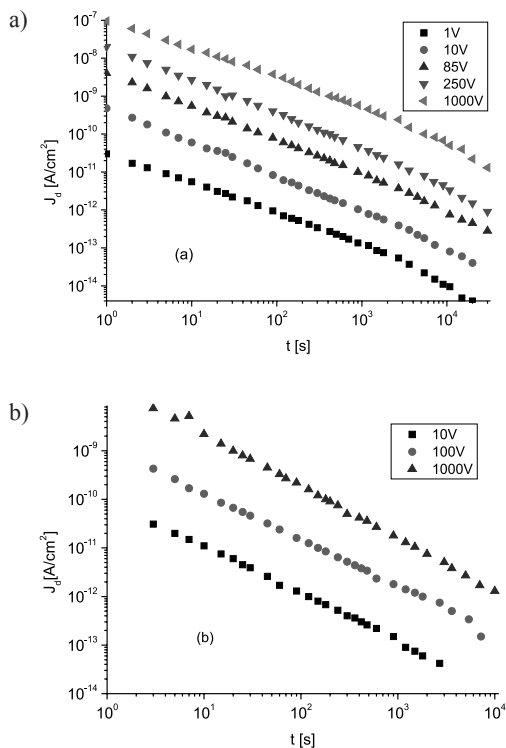


Fig. 2. Depolarization currents ( $J_d$ ) for different poling fields for sample with  $y = 0.47$  measured at 258 K (a) and 77 K (b)

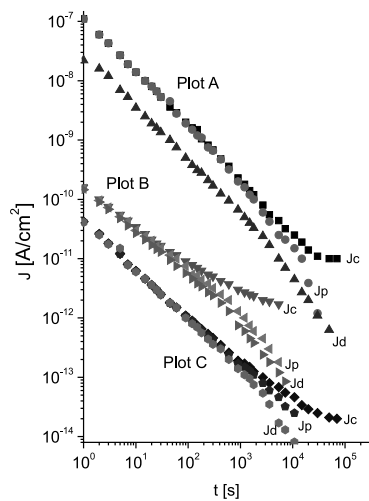


Fig. 3. Charging ( $J_c$ ), polarization ( $J_p$ ) and depolarization ( $J_d$ ) current densities for sample with  $y = 0.47$ . Plot A: temperature 298 K, poling field 5 kV/cm; plot B: temperature 453 K, poling field 0.02 kV/cm; plot C: temperature 298 K, poling field 0.02 kV/cm

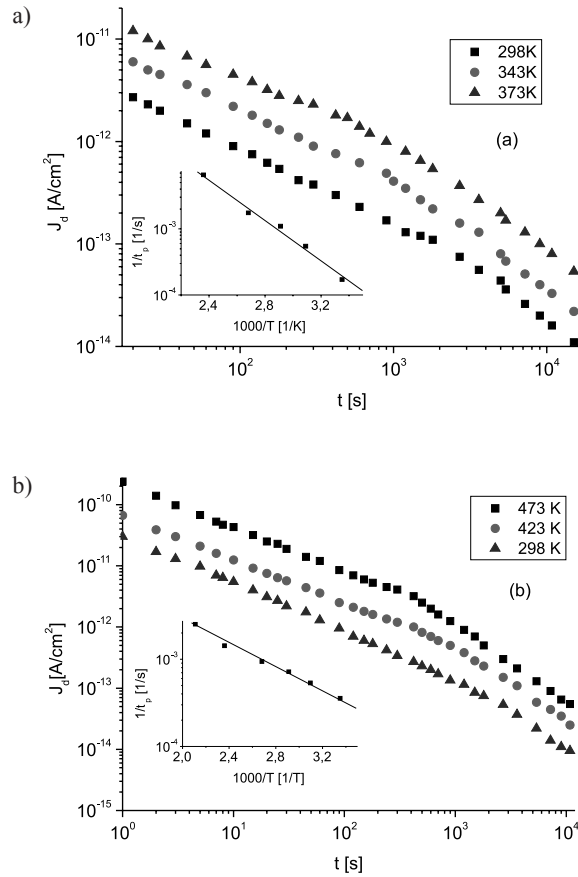


Fig. 4. Depolarization current density ( $J_d$ ) under low poling field (0.02 kV/cm) at different temperatures for samples with  $y = 0.47$  (a) and  $y = 0.43$  (b). The insert shows the  $\log 1/\tau_p$  vs.  $1000/T$  dependence

## References

- [1] Rabe K.M., Dawber M., Lichtensteiger C., Ahn C.H., *Modern physics of ferroelectrics: essential background*, [in:] Rabe K.M., Ahn C.H., Triscone J-M. (Eds.), *Physics of Ferroelectrics A Modern Perspective*, Springer, Berlin–Heidelberg–New York 2007, 1-30.
- [2] Paruch P., Giamarchi T., Triscone J-M., *Nanoscale Studies of Domain Walls in Epitaxial Ferroelectric Thin Films*, [in:] Rabe K. M., Ahn C. H., Triscone J-M. (Eds.): *Physics of Ferroelectrics A Modern Perspective*, Springer, Berlin, Heidelberg, New York 2007, 339-360.
- [3] Carl K., Härdtl K.H., *Electrical After-Effects in Pb(TiZr)O<sub>3</sub> ceramic*, *Ferroelectrics*, vol. 17, 1978, 473-486.

- [4] Kircher O., Bohmer R., *Aging, rejuvenation and memory phenomena in a lead-based relaxor ferroelectric*, Eur. Phys. J., vol. 26, 2002, 329-338.
- [5] Osak A., *Relaxation currents in morphotropic region of  $Pb[(Fe_{1/3}Sb_{2/3})_xTi_yZr_z]O_3$  ferroelectric ceramics*, Phase Transitions, vol. 86 (9), 2012, 1-6.
- [6] Shiguang Yan, Chaoling Mao, Genshui Wang, Chunhaua Yao, Fei Cao, Xilian Dong, *Temperature and voltage stress dependent dielectric relaxation process of the doped  $Ba_{0.67}Sr_{0.33}TiO_3$  ceramics*, Applied Physics Letters, vol. 103, 2013, 112908.
- [7] Jonscher A.K., *Dielectric relaxation in solids*, Chelsea Dielectric Press, London 1983.
- [8] Tosima S., Nishikawa M., *Critical field variation for domain wall motion in ferroelectric/ferroelastic  $Gd_2(MoO_4)_3$* , J. Appl. Phys., vol. 48, 1977, 3169-3170.
- [9] Thomas N.W., *A new framework for understanding relaxor ferroelectrics*, J. Phys. Chem. Solids, vol. 51, 1990, 1419-1431.
- [10] Dissado L.A., Hill R.M., *Dielectric behaviour of materials undergoing dipole alignment transitions*, Phil. Mag. B, vol. 41, 1980, 625-642.
- [11] Jonscher A.K., Jurlewicz A., Weron K., *Stochastic schemes of dielectric relaxation in correlated cluster systems*, Contemporary Physics, vol. 44, 2003, 329-339.
- [12] Ngai K.L. White C.T., *Frequency dependence of dielectric loss in condensed matter*, Phys. Rev. B, vol. 20, 1979, 2475-2486.
- [13] Maraton P., Elsässer, *Switching of substitutional-iron oxygen vacancy defect complex in ferroelectric  $PbTiO_3$  from first principles*, Phys. Rev. B, vol. 83, 2011, 020106.
- [14] Jakes P., Erden E., Eichel R.A., Li Jin, Damjanowic D., *Position of defects with respect to domain walls in  $Fe^{3+}$ -doped  $Pb[Zr_{0.52}Ti_{0.48}]O_3$  piezoelectric ceramics*, Appl. Phys. Letts, vol. 98, 2011, 072907.
- [15] Osak A.P., Ptak W.S., Osak W., Strzałkowska C., *Dielectric and electric properties of polycrystalline  $Pb[(Fe_{1/3}Sb_{2/3})_xTi_yZr_z]O_3$* , Ferroelectrics, vol. 154, 1994, 247-252.